The 1.58 μm transparency window of methane (6165-6750 cm-1): empirical line list and temperature dependence between 80 K and 296 K

Le Wang, Samir Kassi, A. Liu, S. Hu, Alain Campargue

Elsevier Editorial System(tm) for Journal of Quantitative Spectroscopy and Radiative Transfer

Manuscript Draft

Manuscript Number:

Title: The 1.58 micron transparency window of methane (6165- 6750 cm-1): empirical line list and temperature dependence between 80 K and 296 K

Article Type: Full Length Article

Keywords: methane; CH4; CH3D, Titan; absorption spectroscopy; cryogenic cell, CRDS, HITRAN

Corresponding Author: Dr. Alain Campargue, PhD

Corresponding Author's Institution: Université Joseph Fourier/CNRS Grenoble

First Author: Le Wang, Dr

Order of Authors: Le Wang, Dr; Samir Kassi, dr; Anwen LIU, Dr; Shuiming Hu, Dr; Alain Campargue, PhD

Cover Letter

Dear Sir,
Please find attached the paper:
The 1.58 micron transparency window of methane (6165-6750 cm-1):
empirical line list and temperature dependence between 80 K and 296 K

by L. Wang, S. Kassi, A. W. Liu, S. M. Hu, and A. Campargue

that we submit as article in JQSRT.
Regards,
Alain Campargue

Potential reviewers:
Dr. L. Brown: Linda.Brown@jpl.nasa.gov
L.R. Brown,
Jet Propulsion Laboratory, California Institute of Technology, Mail Stop 183-601, 4800 Oak Grove Drive, Pasadena, CA 91109, USA

Dr. Sieghard Albert
address:Dr. Sieghard Albert
Physical Chemistry ETH Hönggerberg - HCI E233 CH-8093 Zürich
tel: +41-44-632 79 18 fax: +41-44-632 10 21
albert@ir.phys.chem.ethz.ch

Dr. Vincent Boudon
Institut Carnot de Bourgogne (ICB)
UMR 5209 CNRS-Université de Bourgogne
9, Avenue Alain Savary
B.P. 47 870 F-21078 DIJON Cedex FRANCEE
E-mail : Vincent.Boudon@u-bourgogne.fr

Research Highlights

The weak absorption spectrum of methane was recorded near 1.58 μm by CRDS at 80K

A list of 12268 transitions at 80 K has been constructed

The temperature dependence of the absorption was determined

The WKC (Wang Kassi Campargue) line list has direct applications in planetary science

The CH_3D contribution to the absorption is important

The 1.58 μm transparency window of methane (6165- 6750 cm^{-1}): empirical line list and temperature dependence between 80 K and 296 K

L. Wang[*], S. Kassi[*], A. W. Liu[*&], S. M. Hu[&], and A. Campargue[*1]

[*] *Laboratoire de Spectrométrie Physique (associated with CNRS, UMR 5588), Université Joseph Fourier de Grenoble, B.P. 87, 38402 Saint-Martin-d'Hères Cedex, France.*
[&] *Hefei National Laboratory for Physical Sciences at Microscale, University of Science and Technology of China, Hefei, 230026, China.*

1st October 2010

Number of figures: 13

Number of Tables: 2

Running Head: *The 1.58 μm CH_4 transparency window at 80 K*

Keywords: *methane; CH_4; CH_3D, Titan; absorption spectroscopy; cryogenic cell, CRDS, HITRAN;*

[1] Corresponding author: Alain. Campargue@ujf-grenoble.fr

Abstract

The empirical line parameters of 12268 transitions of methane at 80 K have been constructed for the 1.58 μm transparency window (6165-6750 cm^{-1}). This line list, WKC, which is of particular interest for several planetary applications, was obtained from high sensitivity spectra recorded by CW-Cavity Ring Down Spectroscopy at low temperature. By comparison with a spectrum of CH_3D recorded separately by Fourier Transform Spectroscopy at low temperature (90-120 K), most of the transitions of monodeuterated methane, CH_3D, in "natural" abundance in the sample were identified. The CH_3D relative contribution in the considered region is observed to be much larger at 80 K than at room temperature. In particular, CH_3D is found strongly dominant in a narrow spectral window near 6300 cm^{-1} corresponding to the highest transparency region.

Using a similar line list constructed at room temperature (A. Campargue, L. Wang, A. W. Liu, S. M. Hu and S. Kassi, Chem. Phys., 373 (2010) 203–210), the low energy values of the transitions observed both at 80 K and at room temperature were derived from the variation of their line intensities. The good quality of the obtained empirical low energy values is demonstrated by the marked propensity of the empirical low *J* values of the CH_4 transitions to be close to integers. The WKC line lists at 80 K and room temperature provided as Supplementary Material allow one accounting for the temperature dependence of methane absorption between these two temperatures. The importance of the 80 K line list for the study of Titan and other methane containing planetary atmospheres is underlined and further improvements are proposed.

1. INTRODUCTION

In a recent contribution [1], we have reported the construction of an empirical list of more than 16000 transitions for methane at room temperature (RT) in the 1.58 μm transparency window (6165- 6750 cm^{-1}). The spectra were recorded by high sensitivity Cavity Ring Down Spectroscopy (CRDS) with the help of 27 fibered distributed feedback (DFB) lasers [2]. The intensity values span over six orders of magnitude from 1.6×10^{-29} to 2.5×10^{-23} cm/molecule. The achieved sensitivity (noise equivalent absorption α_{min}~3×10^{-10} cm^{-1}) allowed us to measure line intensities which are three orders of magnitude smaller than the intensity cut off of the HITRAN [3] line list of methane (4×10^{-26} cm/molecule). The number of measured transitions was increased from 2126 in HITRAN to 16223.

Similar performances could be achieved at liquid nitrogen temperature (LNT) by combining a specifically designed cryogenic cell with the CW-CRDS technique [4]. In Ref. [5], we reported the analysis of the central section of the transparency window (6289-6526 cm^{-1}) region at LNT and RT because it corresponds to the $3\nu_2$ band of CH_3D which is of particular interest for planetary studies. The present contribution is devoted to the completion of the coverage of the transparency window between 6165 to 6750 cm^{-1} and to the construction of the corresponding line list at low temperature. By combining the RT line list of Ref. 1 and the present LNT line list, it is possible to use the so called “two temperature” method to calculate the empirical lower state energies of the transitions, which govern the temperature dependence of the line intensities. The “two temperature” method consists in deriving the low energy levels from the ratio of the intensities of the transitions in common in the LNT and RT spectra. This method was successfully applied to the high absorbing regions surrounding the considered transparency window [6-11] and also to the region of the $3\nu_2$ band of CH_3D [5].

Considering the variation of the CH_3D/CH_4 relative abundance in the various sources of methane on Earth [12] and in planetary atmospheres [13], the discrimination of the CH_3D and CH_4 transitions in the spectrum of methane is a perquisite to satisfactorily account for the transmission in the 1.58 μm window. Apart for the $3\nu_2$ band, many additional CH_3D lines were identified in the RT spectrum [1]. Their identification was based on a comparison to recent FTS recordings of CH_3D spectra performed at USTC (Hefei, China) with long absorption path lengths [1, 5]. An important result obtained in Ref. 1 is the quantitative evaluation of the CH_3D contribution to the absorption at room temperature. From simulations

of the CH_3D and methane spectra at low resolution, the CH_3D isotopologue in "natural abundance" was found to contribute by up to 25% of the absorption in some spectral sections.

Due to the strong temperature dependence of the line intensities, it is sometimes difficult to use the CH_3D spectrum at RT to identify the CH_3D transitions in the LNT spectrum of methane. This is why, in the present work, a FTS spectrum of CH_3D was recorded at low temperature. After the description of the line list construction (Section 2), we will present the procedure followed to identify the CH_3D lines (Section 3). Then the "two temperature" method will be systematically applied to derive the lower state energy of both CH_4 and CH_3D transitions (Section 4). Finally, possible improvements and applications of the obtained line lists will be discussed in Section 5.

2. EXPERIMENT DETAILS AND CONSTRUCTION OF THE LINE LIST AT 80 K

The cryogenic cell which has been specifically designed for CW-CRDS has been described in details in Refs.[4-6]. The cryostat is a 1.42 m long hollow cylinder both filled and completely surrounded by the sample gas volume. The distance between the high reflective mirrors and the cryostat ends is about 0.5 cm. Instead of the usual piezoelectric actuator that modulates the optical cavity length in standard CW-CRDS, a Mode by Mode CRDS acquisition scheme was preferred [4]. The spectra were recorded using the same series of DFB lasers diodes than for the RT spectra [1]. A fast (200 Hz) triangular current modulation was applied to the DFB laser while its temperature was slowly ramped from -10 to 60°C within about 1 hour allowing for a spectral coverage of about 35 cm^{-1}. The current modulation leads to a frequency excursion of about 150 MHz, i.e. slightly more than the Free Spectral Range of our cavity (106 MHz). The average ring-down repetition rate was close to 500 Hz.

A typical value of 3×10^{-10} cm^{-1} was obtained for the noise equivalent absorption [4].

During the recording of both the RT and LNT spectra, the pressure, measured by a capacitance gauge and the ringdown cell temperature were monitored. The LNT spectra were recorded at 1.0, 5.0 and 10.0 Torr. The gas temperature in the cryogenic cell was calculated to be 82 K from the Doppler profile of several tens of lines [4] and 79.6 K from the intensity distribution of the $3\nu_2$ band of CH_3D [5]. The value of 80±2 K is what we refer to as "liquid nitrogen temperature" (LNT).

Each 35 cm^{-1} wide LNT spectrum recorded with one DFB laser was calibrated against the corresponding RT spectrum. The RT spectra were themselves calibrated using the positions values provided in the HITRAN database [3] or a high sensitivity FTS spectrum

recently recorded in Reims [14]. The precision of the obtained wavenumber calibration estimated from the dispersion of the wavenumber differences is 1×10^{-3} cm^{-1}.

The same procedure as described in Ref. 5 was followed to construct the line list. The line intensity, S_{ν_0} (cm/molecule), of a rovibrational transition centred at ν_0, was obtained from the integrated absorption coefficient, A_{ν_0} (cm^{-2}/molecule):

$$A_{\nu_0}(T) = \int_{line} \alpha_\nu d\nu = S_{\nu_0}(T) N \qquad (1)$$

where:

ν is the wavenumber in cm^{-1},

$\alpha(\nu)$ is the absorption coefficient in cm^{-1},

and N is the molecular concentration in molecule/cm^3 obtained from the measured pressure value: $P = NkT$.

The mode by mode scheme adopted for the acquisition of the CRDS spectra at LNT [4], leads to a reduced number of data points defining each line profile: the full profile is described by about six points separated by the Free Spectral Range of the cavity (106 MHz). This reduced number of data points doesn't prevent a satisfactory fitting of the profile as it is compensated by the extreme precision on the corresponding frequencies separated by exactly the FSR.

An interactive multi-line fitting program was used to reproduce the spectrum [15]. A Voigt function of the wavenumber was adopted for the line profile as the pressure self broadening has a significant contribution: at 80 K and 10 Torr, the self broadening (HWHM 2.6×10^{-3} cm^{-1} [16]) is about half the Doppler broadening (HWHM 5.0×10^{-3} cm^{-1}). The HWHM of the Gaussian component was fixed to its theoretical value for $^{12}CH_4$. In the case of blended lines or lines with low signal to noise ratios, the Lorentzian HWHM was also constrained to the average value obtained from nearby lines.

The average density of lines is more than 20 lines per cm^{-1}. This high density and frequent overlapping of the lines made the fitting of the spectrum a very laborious task. Fig. 1 shows an example of comparison between the measured and fitted spectra. Some differences between the observed and simulated spectra are noted. They are partly due to the small sections of warm gas lying between the ends of the cryostat and the supermirrors (see below).

The complete line list at LNT was obtained by gathering the line lists corresponding to the different DFB laser diodes. The final LNT dataset consists of 12268 lines with intensity values ranging from about 6×10^{-30} to 7×10^{-24} cm/molecule for methane in natural abundance

at 80 K. The overview of the RT [1] and LNT line lists is presented in Fig. 2. The minimum value of the line intensities is on the order of 6×10^{-30} i.e. about a factor 10 lower than at RT. This results of the increase of the peak depths of the line due the narrowing by a factor of two of the line intensities at 80 K and to the increase by a factor of 4 of the molecular density at 80 K (at a given pressure value).

The change induced by cooling from RT and LNT is considerable both at high resolution (see for instance Figs. 2, 3 and 6 of Ref. 5) and low resolution. We present in Fig. 3 an overview comparison of the low resolution spectrum absorption spectrum of methane (P = 1.0 Torr) simulated from the line lists at 296 K and 80 K. The spectra were obtained by affecting a normalized Gaussian profile (FWHM = 10.0 cm^{-1}) to each line. It is important to note that the region of highest transparency is significantly shifted to lower energy at 80 K. This is partly due to a strong decrease of the intensities of the lines in the 6200-6300 cm^{-1} region which corresponds to high J transitions of the R branches of the highest energy bands of the tetradecad.

3. IDENTIFICATION OF THE CH_3D TRANSITIONS

The quantitative evaluation of the CH_3D contribution to the absorbance in the considered region is important because the CH_3D/CH_4 relative abundance (and then the opacity) varies significantly depending on the considered planetary atmospheres [13]. As a consequence of the considerable difference of the CH and CD stretching frequencies, the second overtone of the CD stretch of CH_3D, $3\nu_2$, falls in the center of the transparency window. This band was used to determine the D/H ratio in Uranus [17], Neptune [18] and Titan [19,20]. In its most recent version, the HITRAN line list for methane includes the line parameters of the $3\nu_2$ band as obtained 25 years ago from FTS spectra recorded with a highly enriched CH_3D sample [21-23]. Taking into account the relative abundance factor adopted in HITRAN (6.15×10^{-4}) [3], the $3\nu_2$ band of CH_3D has line intensities ranging between 4.3×10^{-27} and 2.5×10^{-26} cm/molecule. These values are below the 4×10^{-26} cm/molecule intensity cut off corresponding to the main isotopologue but well above of our sensitivity threshold. Practically all the $3\nu_2$ transitions of CH_3D listed in the HITRAN database [3] were identified in our RT and LNT spectra of methane in "natural" abundance [1,5]. An important result of Ref. 1 is the evidence of a systematic 18 % deviation of the CH_3D intensities in our methane spectra compared to HITRAN values. This apparent discrepancy was explained [1] by the difference between the CH_3D/CH_4 abundance ratio in our sample (about 5×10^{-4}) and the relative abundance adopted in HITRAN (6.15×10^{-4}). The evidenced 18 % difference

coincides with the usual value of CH_3D depletion in "natural gas" on Earth [12] and leads to a CH_3D abundance in our sample (~5×10^{-4}) very close to the value in Titan atmosphere [24-26].

RT spectrum

As mentioned in the Introduction, the CH_3D lines present in the RT line list were previously identified in Refs. [1,5] by comparison with our FTS spectra of CH_3D. Apart for the $3\nu_2$ transitions of CH_3D listed in the HITRAN database, a high number of additional CH_3D lines were found. They are marked by "D" in the RT line list attached as Supplementary Material of Refs. [1,5]. Also some lines (marked with H/D) were found to have a significant contribution of both CH_3D and CH_4. All the other lines were believed to be due to $^{12}CH_4$ (or $^{13}CH_4$) and are marked with "H" in the RT list [1,5].

LNT spectrum

The identification of the CH_3D transitions in the LNT spectrum is more difficult. Apart for the $3\nu_2$ transitions which are rotationally assigned, the temperature dependence of the methane line intensities is unknown. In Ref. 5 dedicated to the $3\nu_2$ region, we decided to transfer the species determination from the RT line list to the LNT line list: if the difference, δ, of the centres of lines observed in the RT and LNT CRDS spectra differed by less than 0.002 cm^{-1}, the two lines were believed to correspond to the same transition and then to the same species. Although the chosen 0.002 cm^{-1} value is very strict (it corresponds to one fifth of the FWHM Doppler width at 80 K), this method using as only criterion the line centre values may lead to some errors in the (few) cases when a CH_4 line observed at RT has a much weaker intensity at LNT and is blended with a CH_3D line which dominates at LNT. Another drawback is that nearly 60 % of the lines (all weak or very weak) observed at LNT but unobserved at RT were deprived of isotopologue determination. This is in particular the case in the region near 6300 cm^{-1} where CH_3D transitions are completely obscured in the RT spectrum by strong CH_4 transitions which vanished at LNT revealing a high number of CH_3D lines.

In the present work, a reliable identification of most of the CH_3D lines was made possible because a low temperature (90 and 120 K) FTS spectrum of CH_3D was recorded for this purpose at USTC Hefei. The CH_3D sample (stated purity of 99%) was purchased from Sigma-Aldrich. The 21 cm long oxygen-free copper cell was attached to the cold head of a closed-cycle cryostat (Janis SHI-4-5). Two BaF2 windows were adopted to seal the cell with indium wire. A LakeShore 331S controller was used to control the heating current in a wire attached to the cold head. In this way, the temperature can be adjusted in the range of 70-

300K with 0.2 K accuracy. The temperatures in the middle and end of the cell were monitored by two platinum resistance sensors. The measured temperature difference was less than 1.5 K. The high-resolution spectra of CH_3D were recorded with a Bruker IFS 120HR Fourier transform spectrometer (Hefei, China). The entire optical path was evacuated to avoid the atmospheric absorption. A tungsten source, a Ge detector, and a CaF2 beam-splitter were used. The unapodized spectral resolution was 0.015 cm^{-1}. The line positions were calibrated using H_2O lines listed in the HITRAN database [3].

In spite of a short absorption path length, many CH_3D transitions were detected in addition to the $3\nu_2$ transitions. Fig. 4 shows an overview comparison of the FTS spectra of CH_3D at 120 K and RT. The $3\nu_2$ band is accompanied by a number of additional lines around 6300 cm^{-1} which are particularly important as they contribute to the absorption in the spectral section of highest transparency.

The identification of the CH_3D transitions in the CRDS methane spectrum at LNT was then safely performed by comparison to this low temperature FTS spectrum taking into account both the positions and intensities. Fig. 5 shows a spectral section near 6296 cm^{-1} where most of the lines observed at 80 K are unambiguously attributed to CH_3D while they are obscured by much stronger CH_4 lines in the RT spectrum.

As illustrated in Fig. 5, in spite of the small relative abundance of CH_3D in the CRDS spectrum (~5×10^{-4}), the sensitivity of the FTS spectrum of a highly enriched CH_3D sample is not sufficient to allow for the identification of the very weak CH_3D lines. Considering the noise level of the FTS spectrum, we estimate to be 2×10^{-27} cm/molecule the intensity threshold of the CH_3D lines in the LNT CRDS spectrum which could be surely attributed to CH_3D. Below this value, the identification of the CH_3D transitions at LNT was based on the position coincidence ($\delta < 0.003$ cm^{-1}) with the FTS spectrum of CH_3D at room temperature. In consequence, the CH_3D label (D) of the lines with intensities lower than 2×10^{-27} cm/molecule is somewhat less reliable than that for the stronger lines. Finally, we affected a D* label indicating a less secure CH_3D identification for the very few transitions which are not observed in the CH_3D FTS spectrum at room temperature and correspond to lines near the noise level in the CH_3D cold FTS spectrum.

In summary, for both RT and LNT CRDS spectra of methane, we have used a FTS spectrum of CH_3D recorded in similar temperature conditions to find all the CH_3D lines at RT and the lines stronger than 2×10^{-27} cm/molecule at low temperature.

Obviously all the lines with intensities larger than 2×10^{-27} cm/molecule which are not CH_3D lines were marked as CH_4 lines. In addition, we transferred the CH_4 identification from the RT linelist: if a line has a centre at LNT which coincides within 0.003 cm^{-1} to a CH_4 line at RT, it was marked as CH_4.

At the end of the procedure, among the 12268 lines measured at LNT, 5671 were assigned to CH_4 (H), 1572 to CH_3D (D, D*) and 450 were found to have a significant contribution of both isotopologues (H/D). The large set of 4575 very weak lines left without species identification represents less than 1 % of the total absorbance in the region and must be attributed in its large majority to CH_4. Table 1 presents the summary of the species identification at RT and LNT both in terms of number of lines and in terms of the corresponding intensities. Note that the total absorbance in the region decreases by almost a factor of 10 by cooling from RT to LNT. This is mainly due to the considerable decrease of the intensities of the high *J* lines of the *R* branches of the high energy bands of the tetradecad below 6250 cm^{-1}. Note that in both lists attached as Supplementary Material, the CH_3D transitions of the $3\nu_2$ band are indicated by a label (3v2).

Fig. 6 shows an overview of the RT and LNT line lists where the CH_3D transitions (those marked with D and D* in the line lists) have been highlighted.

In order to further quantify the CH_3D contribution to the methane absorption in the region, we have included on Fig. 6 (right hand) a low resolution simulation calculated from the CRDS line lists at RT and LNT. The spectra were obtained by affecting a normalized Gaussian profile (FWHM = 10.0 cm^{-1}) to each line. The CH_3D contribution is indicated at both temperatures. Interestingly, the obtained absorbances show that the CH_3D relative contribution is much more significant at LNT than at RT: while it represents at maximum about 25 % of the total absorption near the *Q* branch of the $3\nu_2$ band at 6430 cm^{-1} and in the lowest opacity region near 6320 cm^{-1}, CH_3D is by far the main absorber in the 6250-6350 micro-window of the LNT spectrum. This is mainly due to the reduction of the extension of the rotational structure of the *R* branches of the high energy bands of the tetradecad and of the *P* branches of the $5\nu_4$ band system at low and high energy, respectively, leading a 100 cm^{-1} spectral interval where the remaining absorption is essentially due to CH_3D.

We have superimposed to the low resolution spectra at RT (Fig. 6 upper panel, right hand), a low resolution simulation of the FTS spectrum of CH_3D at RT with intensities scaled in order to match the intensities of the $3\nu_2$ band in our CRDS spectrum. The obtained low resolution spectrum shows that the proportion of "missing" CH_3D lines in the RT list is

important only in the region where the CH_3D lines could not be identified as they are obscured by much stronger CH_4 lines.

In absence of a high sensitivity spectrum of the $^{13}CH_4$ isotopologue, the $^{12}CH_4$ and $^{13}CH_4$ transitions could not be discriminated. The $5\nu_4$ bands of $^{13}CH_4$ are predicted to be affected by an isotopic shift of some tens of wavenumbers compared to the $5\nu_4$ bands of $^{13}CH_4$ [27]. The $^{13}CH_4$ bands being shifted to lower energy i.e. to the region of weaker absorption, the $^{13}CH_4$ relative contribution to the absorbance in the 6350 cm^{-1} region is expected to be larger than the 1.1 % relative abundance of this isotopologue. Nevertheless, this effect is expected to be limited and no comparable to the CH_3D situation.

4. DETERMINATION OF THE LOWER ENERGY VALUES OF THE TRANSITIONS

Following earlier works by Margolis [28], Pierre et al [29], in the high absorbing regions surrounding the presently studied transparency window, we have systematically used the ratio of the line intensities measured at LNT and RT to determine the low energy levels of the transitions in common in the two spectra [5-11]. As a consequence of the large difference between the two temperatures of our recordings, the "two temperature" method was found to be a particularly efficient and robust method to account for the temperature dependence of the methane absorption.

The lower state energy, *E*, of a given transition is related to the ratio of line intensities at two temperatures [6]:

$$\ln\left(\frac{S_{\nu_0}(T_1)Z(T_1)}{S_{\nu_0}(T_0)Z(T_0)}\right) = -E\left[\frac{1}{kT_0} - \frac{1}{kT_1}\right] \qquad (1)$$

where T_0 and T_1 are the RT and LNT, respectively and S_{ν_0} are the corresponding line intensities.

From the values of the partition function at 296 K and 80 K given in HITRAN for $^{12}CH_4$ [3], we obtain $\frac{Z(296\,K)}{Z(80\,K)} = 7.05337$. This value differs by less than 1 % from the value (7.117) adopted in our previous works assuming a $T^{3/2}$ temperature dependence of the rotational partition function [5-11]. Note that the $\frac{Z(296\,K)}{Z(80\,K)}$ value obtained for $^{12}CH_4$ is very close to the corresponding values for $^{13}CH_4$ (7.05346) and CH_3D (7.07757) and the two temperature method can be applied independently of the methane isotopologue.

The automatic association of the lines in the RT and LNT datasets relies on the coincidence of their centers (obviously they should also be assigned to the same isotopologue in the two datasets). As in our preceding contributions [5-11], a strict criterion is chosen to insure that a RT line and a LNT line correspond to the same transition: the difference, δ, of their centres must differ by less than 0.002 cm^{-1}. This value takes into account the average uncertainties on the two line centre determinations and corresponds to one fifth and one tenth of the Doppler width (FWHM) at LNT and RT, respectively. According to this criterion, 4503 and 591 pairs of transitions were found in coincidence for CH_4 and CH_3D, respectively. They are highlighted in the overview plots presented in Fig. 7. Overall, the associated transitions represent 81.5 and 87.9 % of the total absorbance at RT and LNT, respectively.

Using Eq. 1 hereabove, the lower energy values, *E*, were empirically determined. In the case of both $^{12}CH_4$ and $^{13}CH_4$, the rotational energy levels are well separated and the corresponding empirical *J* values can be computed from $J_{emp} = \sqrt{\frac{1}{4} + \frac{E}{B_0}} - \frac{1}{2}$ where B_0= 5.214 cm^{-1} is the $^{12}CH_4$ (and $^{13}CH_4$) ground state rotational constant. The above expression based on a simple rigid rotor approximation is sufficient as the splitting of the tetrahedral multiplets remains small in our range of *J* values (for instance 0.5 cm^{-1} at *J*=12) [30]. Since CH_3D is a symmetric top molecule, the values of the rotational levels are too dense to unambiguously derive empirical values of the *J* and *K* quantum numbers from the derived *E* value. As an example, the CH_3D transitions and the obtained empirical *J* values of the CH_4 transitions are indicated on the RT and LNT spectra displayed in Fig. 8.

In Fig 9, the empirical *J* values are plotted versus the CH_4 line centres. The observed propensity of the empirical *J* values to be close to integers is a good indication of the quality of the obtained results. In Fig. 10, the corresponding histograms are presented both in terms of numbers of lines and of the corresponding sum of their intensities. As usual, [5, 7-10], the contrast between integer and non integer *J* values is more pronounced for the intensities than for the number of lines. This is due to the fact that the uncertainty on the line intensities values (and then on the *J* values) is larger for the weaker lines and then, on average, non integer *J* values correspond to smaller intensities. 70% of the *J* determinations lead to *J* values falling within a ±0.25 interval around integer values.

Our previous studies [5, 7-10] showed that the δ < 0.002 cm^{-1} criterion is too strict in the case of strongly blended or very weak lines and that additional pairs of lines correspond

undoubtedly to the same transitions and should be associated. We decided to relax the coincidence criterion on the line centres and increased it up to 0.003 cm^{-1} which allowed us to derive 812 additional low energy determinations representing 4.7 % of the total absorbance at both LNT and RT. As the derived low energy values of the lines with $0.002 < \delta < 0.003$ cm^{-1} are expected to be less accurate, they are marked (*) in the line lists provided as Supplementary Material.

The complete sets of transitions measured at 80 K and 296 K are provided as two separate WKC (Wang-Kassi-Campargue) line lists: WKC-80K.txt and WKC-296K.txt. They include the species identification, the *E* values of the lower state for the pairs of associated transitions, together with the empirical *J* values for the CH_4 isotopologues. Table 2 gives a sample of the LNT line list.

Distortion of the high empirical J values

The histograms relative to the number of CH_4 lines and to their intensities at RT (Fig. 10 upper and middle panel, respectively) show that the integer-non integer alternation disappears above *J*=10 and that the obtained empirical *J* values distribution sharply decreases above this value. Such behavior was already noted in our previous studies but is much more pronounced in the presently investigated region as high *J* transitions of the strong bands of the tetradecad are sufficiently strong to be detected at 80 K below 6300 cm^{-1}. A possible explanation of the appearance of the histograms for high *J* values is the weakness of the corresponding transitions in the low temperature spectrum which may lead to larger uncertainties on the retrieved intensity values and then on the J_{emp} values. For instance, the intensity of a *J*=11 transition is divided by about a factor 1075 by cooling from 296 K to 80 K. Nevertheless, larger uncertainties on the intensities would lead to a random dispersion of the empirical *J* values around integer values while a careful examination of Fig. 11 shows that around *J*=10, the empirical *J* values appear systematically shifted down to about 9.6.

Such a systematic effect is in fact due to the small sections of warm gas lying between the ends of the cold jacket and the windows of the cryogenic cell [4]. The external stainless steel cylinder is 1.4 m long, has a $\Phi = 6.3$ cm diameter while the cryostat is made of two co-axial tubes (Φ = 1.6 and 2 cm) joined at the ends by two rings. The distance between the cryostat ends and the high reflective mirrors is only 6 mm (at RT). Inside the inner tube, the gas sample rapidly equilibrates to the cryostat temperature but in the intermediate space between the cryostat and the mirrors, the gas temperature is expected to increase from 80 K to a value approaching the room temperature. Compared to a cryognic cell with a uniform low

temperature, this warmer section of gas leads to an overestimation of the intensity of the high *J* transitions and then an underestimated empirical value of *J*. Taking into account the 4 mm contraction of the cryostat at LNT, the total pathlength ouside the cryostat is 16 mm i.e. only 1.1 % of the total path length. This temperature gradient has a negligible effect for *J* values lower than 9 but for higher *J* values, the situation is different due to the steep decrease of the LNT line intensities. For instance, a *J*=11 lines has its intensity divided by more than 3 orders of magnitude at 80 K compared to RT and the 1% section of warm gas is expected to have a larger contribution to the measured intensity than the 99 % section of the cell at 80 K.….

In order, to quantify this effect, we have considered a simple model assuming a linear dependance of the gas temperature between 80 K at the ends of the cryostat and 290 K on the mirrors (the measured temperature of the outside cylinder is about 290 K). Fig. 11 shows the ratio, *r*, of the line intensities for a cell with such a temperature gradient and a cell at an uniform temperature of 80 K. The obtained curve (plotted in logarithmic scale) shows that, while the warm gas has practically no impact below *J*= 9, it begins to dominate the absorption at *J*= 10. Using the correction factor, *r*, on the line intensities, the deviation of the retrieved *J* value from their real value can be computed. It leads to the curve included in Fig. 11 which gives for *J*= 10, an apparent *J* value very close to the value of 9.6 estimated from Fig. 11 . The apparent *J* values increase very slowly above *J*= 10 with an asymptote around J_{emp}= 11 in good agreement with the histograms of Fig. 10.

It is worth underlining that high *J* lines with a distorted lower *J* values and therefore inaccurate temperature dependence are completely negligible at low temperature and has a significant contribution at room temperature only in the small 6200-6250 cm^{-1} interval where are located the high *J* lines of the R branches of the tetradecad (see Fig. 9). The experimental evidence of the distortion of the very weak intensities of the high *J* lines illustrates the high dynamics on the intensity values (more than 4 decades) which can be measured with our CW-CRDS spectrometer.

5. DISCUSSION

Comparison with the GOSAT line list

In relation with the "Greenhouse Gases Observing Satellite" (GOSAT) project [31], a line list has become recently available for methane at room temperature in the 5550–6236 cm^{-1} range [32]. This line list was constructed from FTS spectra recorded with a coolable White-type cell in a large variety of temperature and pressure conditions. The intensity cut off of the GOSAT line list (about 4×10^{-26} cm/molecule) is two orders of magnitude lower than that of

the Margolis line list [33] included in the HITRAN database in that region and equivalent to that of Brown's list [34] adopted for HITRAN above 6180 cm^{-1}. The GOSAT line list which covers the whole tetradecad from 5550 to 6236 cm^{-1} can be compared to our present results in the 6165-6236 cm^{-1} overlapping region. Fig. 12 shows the considerable gain in terms of sensitivity: the CRDS line list at RT includes1876 transitions while the GOSAT line list is limited to the 437 strongest lines. The additional lines detected by CRDS add 12.7 % to the total GOSAT absorbance in the region. We have also included in this Figure, the overview comparison of the CRDS line list at LNT to the line list previously constructed from spectra recorded by Differential Absorption Spectroscopy (DAS) at LNT [10]. While the intensity cut off of the GOSAT and DAS are similar, the gain in sensitivity is even more pronounced compared to DAS at LNT.

Possible improvements of the line lists

In principle, theoretical analysis may provide valuable information to improve our empirical line list. For instance the empirical values of the lower state energy may be replaced by their exact value when the transitions have been fully assigned on a theoretical basis. Unfortunately, theoretical analyses are very scarce and still in progress in our region. A partial modelling of the tetradecad region on the basis of the GOSAT line list was recently reported [32]. In the 6165-6236 cm^{-1} region overlapping with GOSAT dataset, 73 of the 437 transitions were fully rovibrationally assigned on the basis of theoretical considerations while we measured 1876 lines. The treatment of the 1.58 μm transparency window corresponding to the lowest energy bands of the icosad is particularly challenging. Very recently, Nikitin et al have succeeded in assigning and reproducing about 2000 transitions of our LNT and RT line lists near 6350 cm^{-1} [14]. Although limited to the $5\nu_4$ and $\nu_2+4\nu_4$ band systems of the main isotopologue and even if the data reproduction could not reach the experimental accuracy, the developed effective Hamiltonian approach [14] provides valuable information. In the few cases where the theoretical model predicts several coinciding transitions which were considered as a single line in the line profile fitting of the CRDS spectrum, the single experimental line may be replaced by the several components predicted by the model with the same (experimental) position and the empirical line intensity distributed according to the predicted relative intensities. Although suitable to take advantage of the recent theoretical advances, the proposed improvements (which represent a difficult and laborious task) are expected to lead to marginal changes for most applications.

Note that in Ref. [14], we have compared the rounded empirical *J* values of the lower state with their theoretical values for the 836 lines whose calculated and measured line centres differ by less than 5×10^{-3} cm^{-1}. We obtained an agreement for 87 % of the transitions, which illustrates the reliability of the "two temperature" method.

6. CONCLUSION

The temperature dependence of the methane spectrum in the 1.58 μm transparency window of methane has been determined by applying the two temperature method to CRDS spectra recorded at 80 K and room temperature. This experimental approach has the advantage of completeness i.e. of providing spectroscopic information about the three isotopologues contributing to the spectrum of methane in "natural" abundance ($^{12}CH_4$, CH_3D and $^{13}CH_4$). The two temperature method which applies independently of the isotopic species has proved to be a pragmatic approach fulfilling urgent needs in planetary science while the complete theoretical treatment of the spectrum of these three species is out of reach in the near future. We present in Fig. 13 a comparison of the total absorption to a low resolution simulation of the absorption corresponding to the transitions for which the lower state energy could be derived. Over the whole spectral region, the temperature dependence has been characterized for most of the absorption. Nevertheless, Fig.7 shows that substantial improvements are still needed to identify the weak CH_3D transitions and determine their temperature dependence. This improvement will be particular important near 6250 cm^{-1} where this isotopologue is the main absorber at LNT. For this purpose, we are planning to use DAS to record new CH_3D spectra both at RT and LNT with an increased sensitivity.

The WKC (Wang-Kassi-Campargue) line list at 80 K attached as Supplementary Material is of particular importance for the studies of the giant planets and Titan. For instance, the methane absorption in the considered transparency window is so weak that observations of Titan allow probing the lower atmospheric levels (troposphere) and all the way down to the surface [35, 36]. Our line list has the advantage to correspond to temperature conditions which are close to those existing in Titan atmosphere and thus to limit the temperature extrapolation of the line intensities needed for the radiative transfer models. The present WKC-80K line list has already been compared with the various band models used so far in the analysis of planetary spectra and significant deviations were evidenced [37]. It was also used to account for the 6200-6600 cm^{-1} region of Titan spectra recorded by FTS at the 4-m telescope of Kitt Peak National Observatory at a resolution of 1.2 cm^{-1}. It led to an excellent

match of all CH_4 and CH_3D features and allowed a new derivation of the CH_3D/CH_4 and CO mole fractions on Titan [37].

In the future, planetary applications of the WKC-80K line list would include analysis (or re-analysis) of other objects with atmospheres containing methane, from giant planets (Uranus, Neptune) to exoplanets.

Acknowledgements

This work is part of the ANR project "CH4@Titan" (ref: BLAN08-2_321467) which is a joint effort among four French laboratories (ICB-Dijon, GSMA-Reims, LSP-Grenoble and LESIA-Meudon) to adequately model the methane opacity. The support of the Groupement de Recherche International SAMIA between CNRS (France), RFBR (Russia) and CAS (China) is acknowledged.

Table 1.

Summary of the observations and corresponding intensities of the CH_3D and CH_4 transitions measured by CRDS at 296 and 80 K between 6165 and 6750 cm^{-1}.

	CH_4 (H)	CH_3D (D,D*)	blended (H/D)	Total
	Number of lines			
296 K	13714	1393	1116	16223
80 K	5671+4575 (no mark)	1572	450	12268
	Intensity (cm/molecule)			
296 K	1.29E-21 (99.81%)	1.56E-24 (0.12%)	8.96E-25 (0.069%)	1.30E-21
80 K	1.45E-22 (97.3%) +1.07E-24 (0.72%) (no mark)	2.62E-24 (1.76%)	2.33 E-25 (0.16%)	1.49E-22

Table 2.

Wavenumbers and line strengths of the methane transitions measured at 80 K by CW-Cavity Ring Down Spectroscopy near 6591 cm^{-1}.
This Table is a small section of the WKC-80K list of 12268 transitions between 6165 and 6750 cm^{-1} which is provided as Supplementary Material.

ISO[a]	*T*=80 K		*T*=296 K[1]			
	Center (cm^{-1})	*Intensity* (cm/mol)	*Center* (cm^{-1})	*Intensity* (cm/mol)	*E* (cm^{-1})	J_{emp}
H	6591.1405	1.428E-26	6591.1406	4.289E-27	56.809	2.83
H	6591.1761	7.464E-26	6591.1762	4.283E-26	105.798	4.02
D	6591.2185	9.197E-29	6591.2170	4.790E-28	272.712	
	6591.2554	1.285E-28				
H	6591.2694	7.961E-28	6591.2684	3.157E-27	252.084	6.45
H	6591.2921	1.597E-26	6591.2924	5.138E-26	236.259	6.23
H	6591.3241	1.706E-27	6591.3251	3.185E-26	369.322	7.91
H	6591.4603	2.540E-27				
H	6591.4943	5.741E-27	6591.4954	1.650E-26	227.722	6.11
H	6591.5528	4.794E-27	6591.5518	1.521E-26	235.204	6.22
H	6591.6129	3.305E-28	6591.6129	7.561E-27	384.704	8.08
	6591.6195	1.438E-28				
H	6591.6530	4.021E-27	6591.6526	2.774E-26	293.984	7.01
H	6591.6861	2.819E-26	6591.6862	8.571E-26	231.981	6.17
H	6591.7354	4.068E-29	6591.7376	1.976E-27	441.682*	8.69*
	6591.7641	5.600E-29				
H	6591.7752	1.235E-28	6591.7770	2.100E-27	362.251	7.83
	6591.7873	1.926E-28				
	6591.7958	2.026E-28				
	6591.8038	2.137E-28				
H	6591.8234	1.676E-27	6591.8248	2.255E-26	344.534	7.62
H	6591.8992	5.520E-27	6591.9004	2.445E-27	86.206	3.59
H	6591.9978	2.740E-28	6591.9983	7.041E-27	393.499	8.18
H	6592.0573	1.976E-28	6592.0567	4.640E-27	386.677	8.10
H	6592.0687	5.174E-28	6592.0682	4.161E-26	479.836	9.08

Notes:
[a] Isotopologue: "H" corresponds to both the $^{12}CH_4$ and $^{13}CH_4$ isotopologues while "D" corresponds to CH_3D (see Text).
The low energy values, *E*, were obtained for the transitions whose centre coincides with that of a line observed in the 296 K spectrum ($\delta \leq 0.002$ cm^{-1}). The "*" symbol in the last column marks the lines whose RT and LNT line centres differ by $0.002 < \delta < 0.003$ cm^{-1}.
For CH_4, the empirical *J* values are given in the last column.

References

[1] Campargue A, Wang L, Liu AW, Hu SM and Kassi S. Empirical line parameters of methane in the 1.63-1.48 μm transparency window by high sensitivity Cavity Ring Down Spectroscopy**.** Chem Phys 2010;373:203–10.

[2] Liu AW, Kassi S and Campargue A. High sensitivity CW-cavity ring down spectroscopy of CH_4 in the 1.55 μm transparency window. Chem Phys Lett 2007;447:16-20.

[3] Rothman LS, Gordon IE, Barbe A, Benner DC, Bernath PF et al. The HITRAN 2008 molecular spectroscopic database. JQSRT 2009;110:533-72.

[4] Kassi S, Romanini D, Campargue A. Mode by Mode CW-CRDS at 80 K: Application to the 1.58 μm transparency window of CH_4. Chem Phys Lett 2009;477:17–21.

[5] Wang L, Kassi S, Liu AW, Hu SM and Campargue A. High sensitivity absorption spectroscopy of methane at 80 K in the 1.58 μm transparency window: Temperature dependence and importance of the CH_3D contribution. J Mol Spectrosc 2010;261:41-52.

[6] Kassi S, Gao B, Romanini D, Campargue A. The near infrared (1.30 -1.70 μm) absorption spectrum of methane down to 77 K. Phys Chem Chem Phys 2008;10:4410-19.

[7] Gao B, Kassi S, Campargue A. Empirical low energy values for methane transitions in the 5852-6181 cm^{-1} region by absorption spectroscopy at 81 K. J Mol Spectrosc 2009;253:55-63.

[8] Sciamma-O'Brien E, Kassi S, Gao B, Campargue A. Experimental low energy values of CH_4 transitions near 1.33 μm by absorption spectroscopy at 81 K. JQSRT 2009;110:951–63.

[9] Campargue A, Wang L, Kassi S, Mašát, M and Votava O. Temperature dependence of the absorption spectrum of CH_4 by high resolution spectroscopy at 81 K: (II) The Icosad region (1.49-1.30 μm). JQSRT 2010;111:1141-51.

[10] Wang L, Kassi S, Campargue A. Temperature dependence of the absorption spectrum of CH_4 by high resolution spectroscopy at 81 K: (I) The region of the $2\nu_3$ band at 1.66 μm JQSRT 2010;111:1130-40

[11] Votava O, Mašát M, Pracna P, Kassi S, Campargue A. Accurate determination of low state rotational quantum numbers (J<4) from planar-jet and liquid nitrogen cell absorption spectra of methane near 1.4 micron, Phys Chem Chem Phys 2010;12:3145-55.

[12] Sowers T. Late Quaternary Atmospheric CH_4 Isotope Record Suggests Marine Clathrates Are Stable. Science 2006;311:838-40.

[13] de Bergh C, Lutz BL, Owen T, Maillard JP. Monodeuterated methane in the outer solar system. IV. Its detection and abundance on Neptune. Astrophys J 1990;355:661-66.

[14] Nikitin AV, Thomas X, Régalia L, Daumont L, Von der Heyden P, Tyuterev VIG, Wang L, Kassi S and Campargue A. Assignment of the $5\nu_4$ and $\nu_2+4\nu_4$ band systems of $^{12}CH_4$ in the 6287-6550 cm^{-1} region. JQSRT doi:10.1016/j.jqsrt.2010.08.006

[15] Daumont L, Vander Auwera J, Teffo JL, Perevalov VI, Tashkun SA. Line Intensity Measurements in $^{14}N_2{}^{16}O$ and Their Treatment Using the Effective Dipole Moment Approach: I. The 4300- to 5200-cm^{-1} Region. J Mol Spectrosc 2001;208:281-91.

[16] Ménard-Bourcin F, Ménard J, Boursier C. Temperature dependence of rotational relaxation of methane in the $2\nu_3$ vibrational state by self- and nitrogen-collisions and comparison with line broadening measurements. J Mol Spectrosc 2007;242:55-63.

[17] de Bergh C, Lutz BL, Owen T, Brault J, Chauville J. Monodeuterated methane in the outer solar system. II. Its detection on Uranus at 1.6 microns. Astrophys J 1986;311:501-10.

[18] de Bergh C, Lutz BL, Owen T, Maillard JP. Monodeuterated methane in the outer solar system. IV. Its detection and abundance on Neptune. Astrophys J 1990;355:661-666.
[19] de Bergh C, Lutz BL, Owen T, Chauville J. Monodeuterated methane in the outer solar system. III. Its abundance on Titan. Astrophys J 1988;329:951-55.
[20] Penteado PF, Griffith CA, Greathouse TK, de Bergh C. Measurements of CH_3D and CH_4 in Titan from infrared spectroscopy. Astrophys J 2005;629:L53-L56.
[21] Lutz BL, de Bergh C, Maillard JP. Monodeuterated methane in the outer solar system. I. Spectroscopic analysis of the bands at 1.55 and 1.95 microns. Astrophys J 1983;273:397-409.
[22] Boussin C, Lutz BL, de Bergh C, Hamdouni A. Line intensities and self-broadening coefficients for the $3\nu_2$ band of monodeutrated methane. JQSRT 1998;60:501-14.
[23] Boussin C, Lutz BL, Hamdouni A, de Bergh C. Pressure broadening and shift coefficients for H_2, He and N_2 in the $3\nu_2$ band of $^{12}CH_3D$ retrieved by a multispectrum fitting technique. JQSRT 1999;63:49-84.
[24] Coustenis A, Achterberg R, Conrath B et al. The composition of Titan's stratosphere from Cassini/CIRS mid-infrared spectra. Icarus 2007;189:35-62.
[25] Penteado PF, Griffith CA. Ground-based measurements of the methane distribution on Titan. Icarus 2010;206:345-51.
[26] Bézard B, Nixon CA, Kleiner I, Jennings DE. Detection of $^{13}CH_3D$ on Titan. Icarus 2007;91:397-400.
[27] Nikitin AV, Mikhailenko S, Morino I, Yokota T, Kumazawa R and Watanabe T. Isotopic substitution shifts in methane and vibrational band assignment in the 5560-6200 cm^{-1} region. JQSRT 2009;110:964-73.
[28] Margolis JS. Empirical values of the ground-state energies for methane transitions between 5500 and 6150 cm^{-1}. Appl Opt 1990;29:2295–302.
[29] Pierre G, Hilico JC, de Bergh C. The region of the $3\nu_3$ band of methane. J Mol Spectrosc 1980;82:379–93.
[30] Champion JP, Hilico JC and Brown LR. The vibrational ground state of $^{12}CH_4$ and $^{13}CH_4$. J Mol Spectrosc 1989;133:244–55.
[31] http://gosat.nies.go.jp.
[32] Nikitin AV, Lyulin OM, Mikhailenko SN, Perevalov VI, Filippov NN, Grigoriev IM et al. GOSAT-2009 methane spectral linelist in the 5550–6236 cm^{-1} range. JQSRT 2010; doi:10.1016/j.jqsrt.2010.05.010 |
[33] Margolis JS. Measured line positions and strengths of methane from 5500 to 6180 cm^{-1}. Appl Opt 1988;27:4038–51.
[34] Brown LR. Empirical line parameters of methane from 1.1 to 2.1 μm. JQSRT 2005;96:251-270.
[35] Griffith CA, Owen T, Wagener R. Titan's surface and troposphere, investigated with ground-based, near-infared observations. Icarus 1991;93:362–378.
[36] Tomasko MG, and Smith PH. Photometry and polarimetry of Titan - Pioneer 11 observations and their implications for aerosol properties. Icarus 1982;51:65-95.
[37] de Bergh et al. Implications of a new CH_4 database on the analysis of Titan spectra in the 1.56 μm window. Plan Space Sci 2010 submitted

Figure Captions

Fig. 1.

An example of simulation of the CH_4 spectrum recorded at LNT near 6234 cm^{-1}.

From top to bottom:

Upper panel: Experimental spectrum at LNT (P = 10.0 Torr),

Middle panel: Simulated spectrum resulting from the line fitting procedure (a Voigt profile was affected to each line),

Lower panel: Residuals between the simulated and experimental spectra.

Fig. 2.

Overview comparison of the line lists constructed from the CRDS spectrum of methane at 296 K (upper panel) and 80 K (lower panel) in the 6150-6750 cm^{-1} region.

Fig. 3.

Comparison of the 'low resolution' absorption spectrum of methane (P = 1.0 Torr) simulated from the CW-CRDS line lists at 296 K (short dot) and 80 K (full). The spectra were obtained by affecting a normalized Gaussian profile (FWHM = 10.0 cm^{-1}) to each line.

Fig. 4.

Overview comparison of the FTS spectra of CH_3D (99% stated purity) recorded at 120 K and room temperature in the 6150-6550 cm^{-1} region. The sample pressure and the absorption pathlength were 4.17 Torr of 15 m at room temperature and 47.5 Torr and 21 cm at 120 K. Note the clear reduction of the extension of the P and R branches of the $3\nu_2$ band at 6425 cm^{-1} and that many lines not belonging to $3\nu_2$ are detected in the 6250- 6350 cm^{-1} section.

Fig. 5.

Identification of the CH_3D transitions in the CRDS spectrum of methane at 80 K (middle panel) by comparison to the FTS spectrum of CH_3D recorded at 120 K (lower panel). The room temperature CRDS spectrum of methane at room temperature is displayed on the upper panel with the corresponding room temperature FTS spectrum of CH_3D. In the displayed region, the CH_3D transitions dominate the 80 K spectrum of methane while they are totally obscured by the much stronger CH_4 lines at room temperature (upper panel).

Fig. 6.

Contribution of the CH_3D transitions to the methane absorption between 6150 and 6750 cm^{-1} at room temperature (upper panels) and 80 K (lower panels)

Left hand: the CH_3D transitions have been highlighted in blue.

Right hand: corresponding low resolution simulations (P = 1.0 Torr) obtained from the complete line list (purple) and limited to the CH_3D lines (blue). Note that while CH_3D transitions represent at most 25 % of the absorption at room temperature, it represents most of the absorption at 80 K near 6300 cm^{-1}. On the upper panel, the low resolution FTS spectrum of CH_3D has been superimposed to the CW-CRDS spectrum of methane.

Fig. 7

Overview of the spectrum of CH_3D (left hand) and CH_4 (right hand) between 6150 and 6750cm^{-1} as obtained from the analysis of the CW-CRDS spectra at 296 K (upper panel) and 80 K (lower panel). The transitions for which the lower energy value was derived from the

ratio of the line intensities (δ < 0.002 cm^{-1}) are highlighted with pink and red symbols for CH_3D and CH_4, respectively.

Fig. 8

Comparison of the CW-CRDS spectra of methane at liquid nitrogen temperature (lower panel) and room temperature (upper panel) near 6542 cm^{-1}. The RT and LNT spectra were recorded with pressures of 10.0 and 1.0 Torr, respectively. The few CH_3D transitions observed in the region are marked with "D". The empirical *J* values obtained from the temperature variation of the line intensities are indicated for the CH_4 isotopologue.

Fig. 9

Empirical *J* values of the CH_4 transitions observed between 6150 and 6750 cm^{-1} versus the transition wavenumbers.

Fig. 10

Histograms of the empirical *J* values determined for the CH_4 transitions (step interval of 0.5). The upper panel is relative to the number of lines. In the two lower panels, the corresponding RT and LNT line intensities were added for each step interval. Note that the contrast between integers and non integers is more pronounced in terms of intensities than in terms of number of lines (see Text).

Fig. 11.

Calculated impact on the measured absorption and empirical *J* values of temperature gradient between the end of the cryostat and the super mirrors.

Upper panel: ratio of the measured line intensity to the intensity value corresponding to a cell at a homogeneous temperature (80 K). Note the logarithmic scale adopted for the ratios.

Lower panel: variation of the empirical *J* values obtained neglecting the temperature gradient versus the actual *J* values. The temperature gradient has no effect for *J* values lower than 10.

Fig. 12.

Overview comparison of different line lists in the 6140-6250 cm^{-1} region corresponding to the high energy part of the tetradecad.

Left hand: Room temperature. The GOSAT line list (full circles) is presented superimposed to the CRDS line list [1].

Right hand: Low temperature (80 K). The line list obtained by direct absorption spectroscopy [10] (full circles) is presented superimposed to our CRDS line list.

Fig. 13.

Part of the methane absorption at 80 K for which the temperature dependence has been derived in the 6150-6750 cm^{-1} region. The solid line corresponds to a low resolution simulation (FWHM = 10.0 cm^{-1}) of the methane spectrum at 80 K and 1 Torr while the dashed line corresponds to a similar simulation limited to the lines with lower state energy derived by the "two temperature" method.

Figure(s)

Fig.1

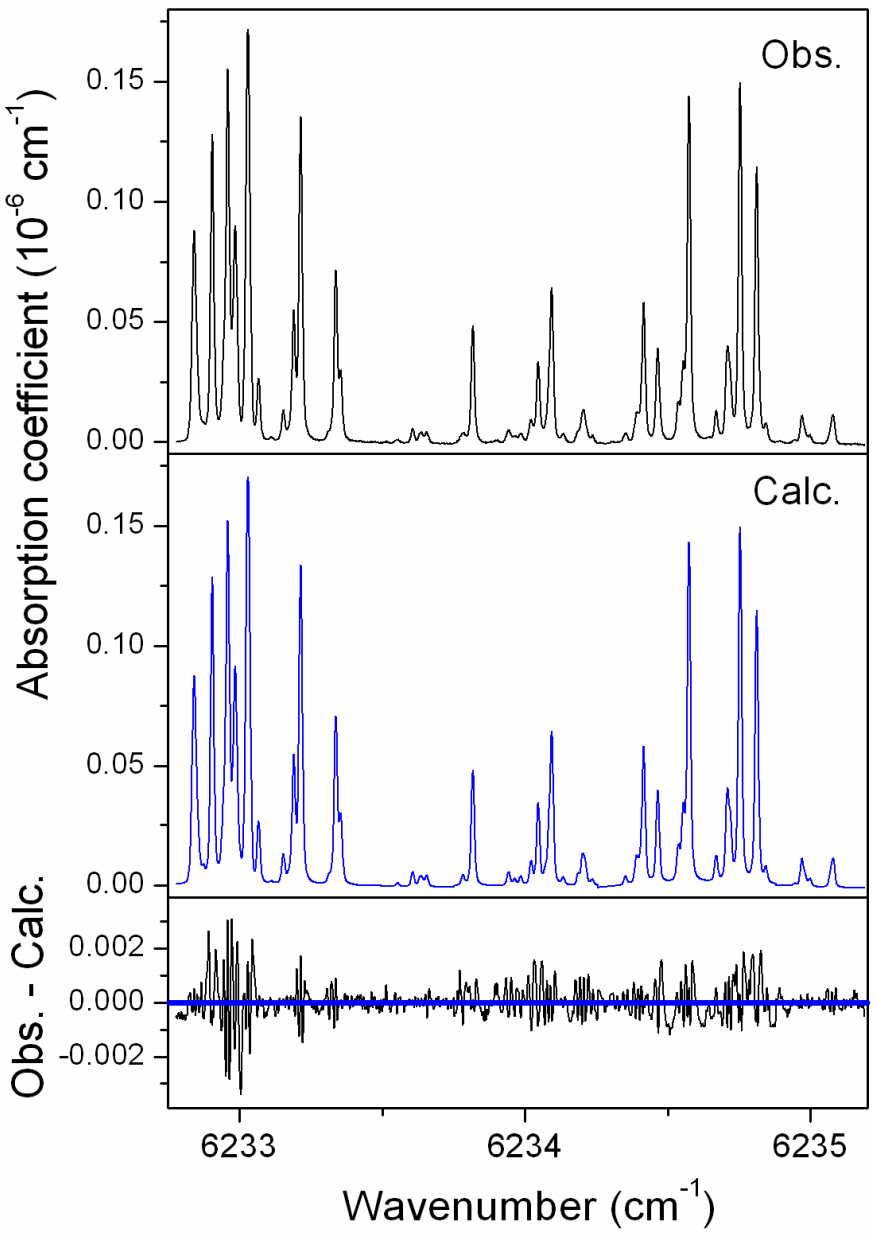

Fig.2

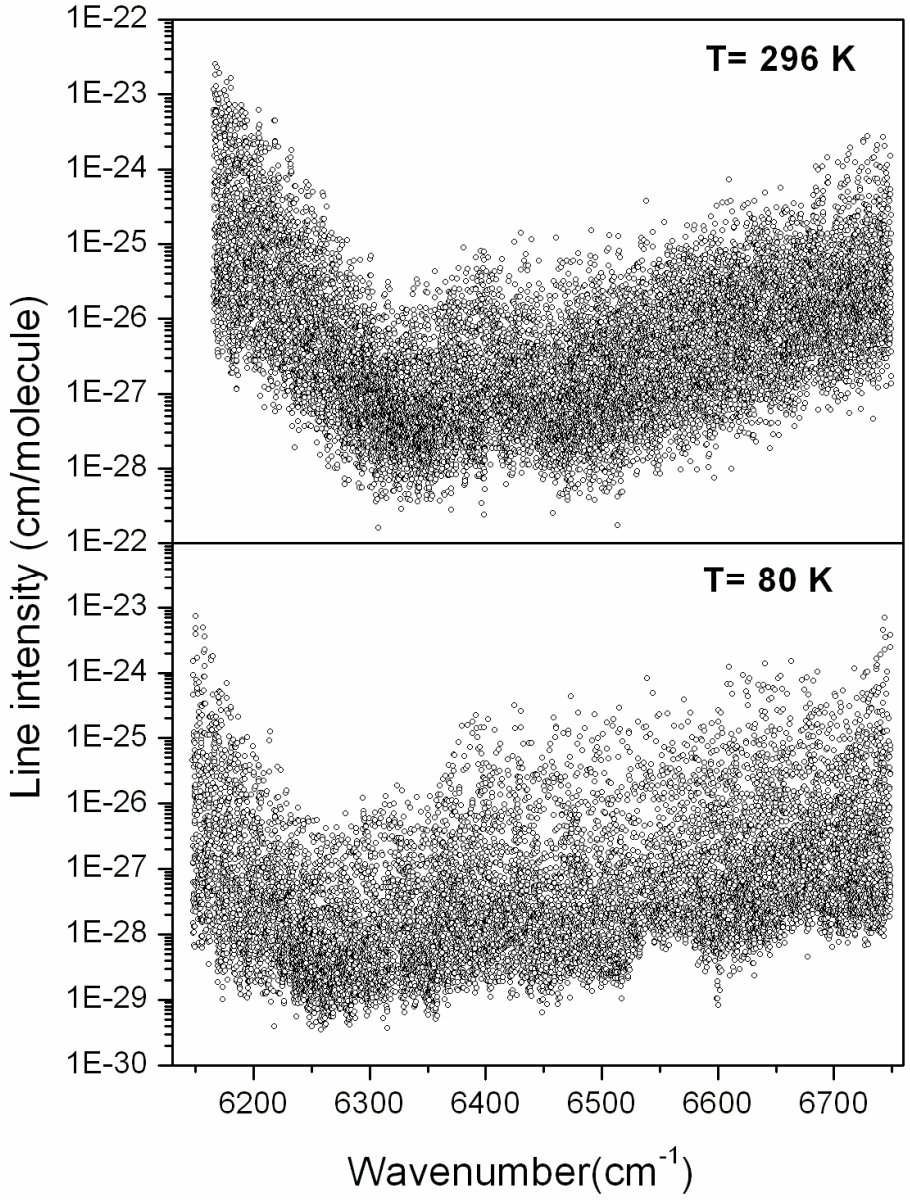
T= 296 K
T= 80 K
Line intensity (cm/molecule)
1E-22
1E-23
1E-24
1E-25
1E-26
1E-27
1E-28
1E-29
1E-30
6200
6300
6400
6500
6600
6700
Wavenumber(cm-1)

Fig.3

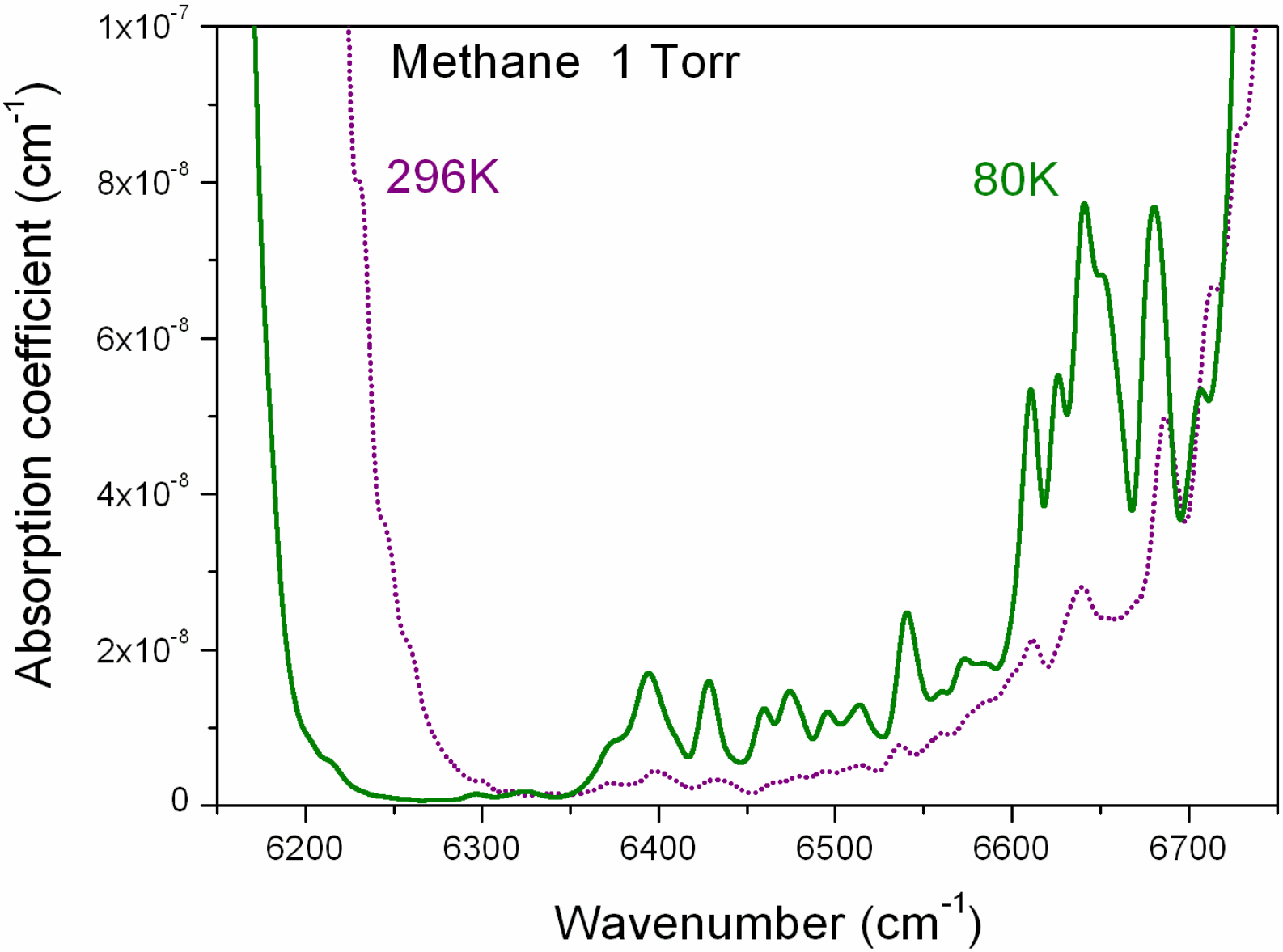
Methane 1 Torr
296K
80K
Absorption coefficient (cm-1)
1x10-7
8x10-8
6x10-8
4x10-8
2x10-8
0
6200
6300
6400
6500
6600
6700
Wavenumber (cm-1)

Fig.4

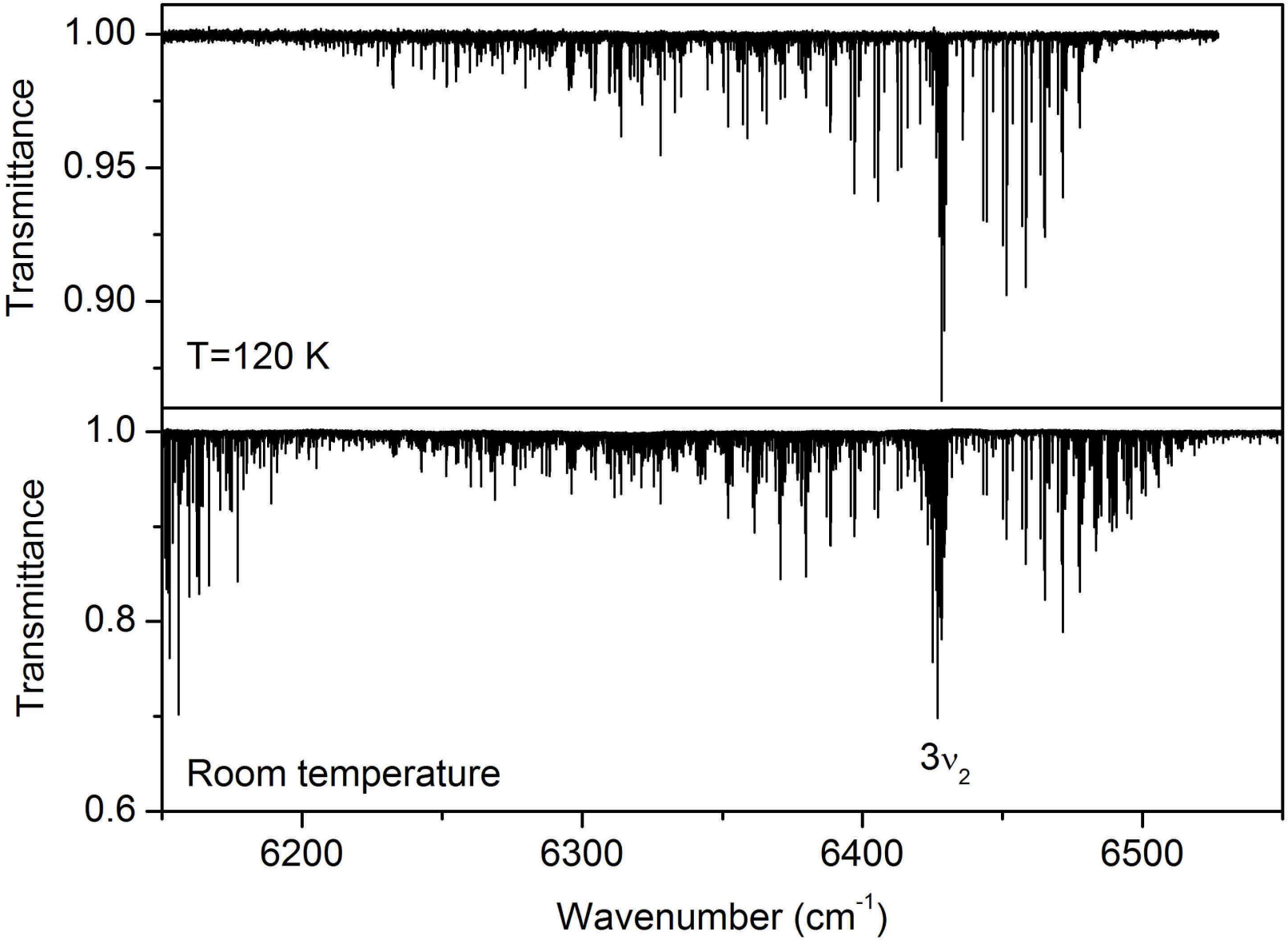
1.00
0.95
0.90
Transmittance
T=120 K
1.0
0.8
0.6
Transmittance
Room temperature
3ν2
6200
6300
6400
6500
Wavenumber (cm-1)

Fig.5

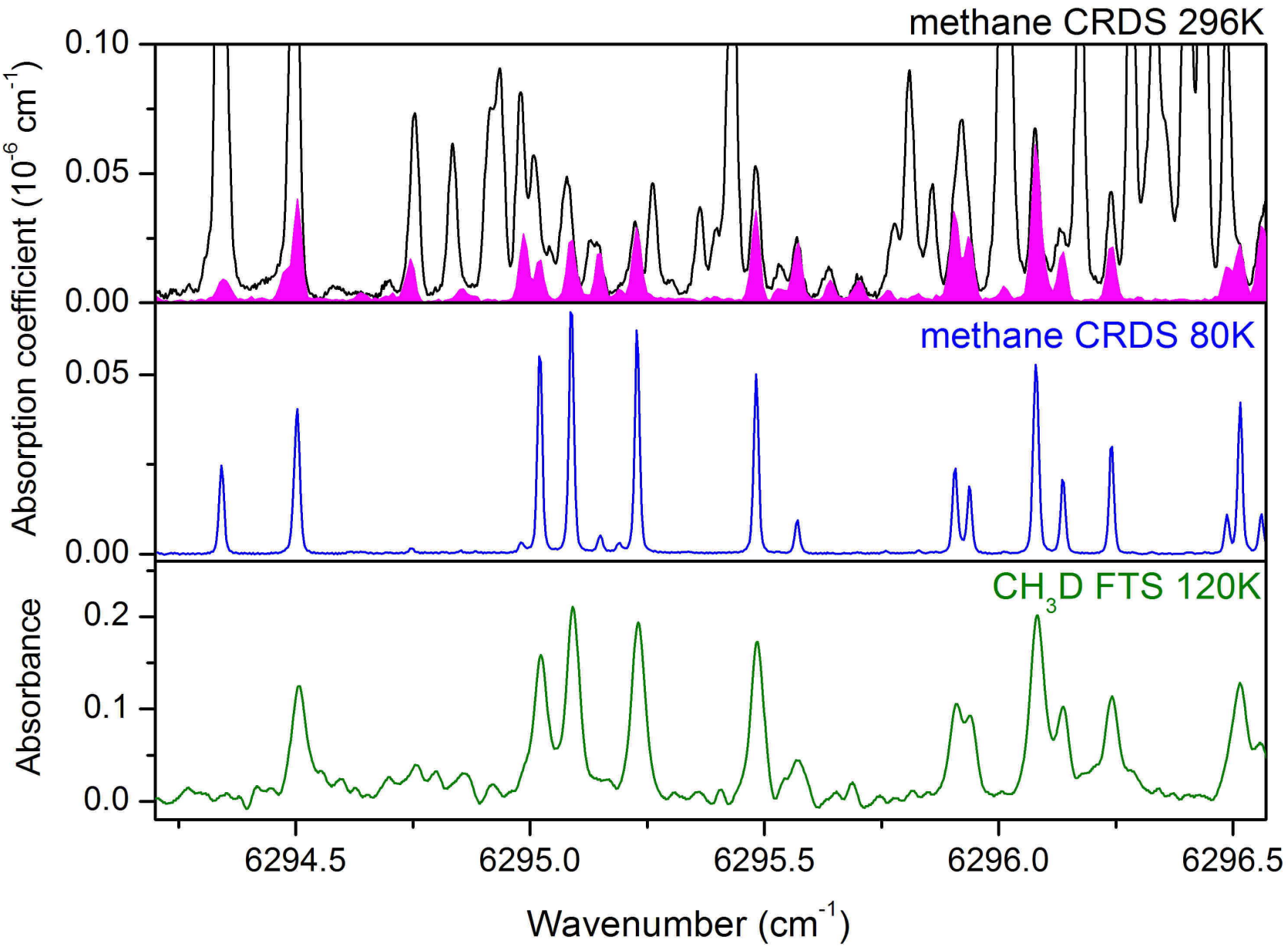
methane CRDS 296K
methane CRDS 80K
CH3D FTS 120K
Absorption coefficient (10-6 cm-1)
Absorbance
0.10
0.05
0.00
0.05
0.00
0.2
0.1
0.0
6294.5
6295.0
6295.5
6296.0
6296.5
Wavenumber (cm-1)

Fig.6

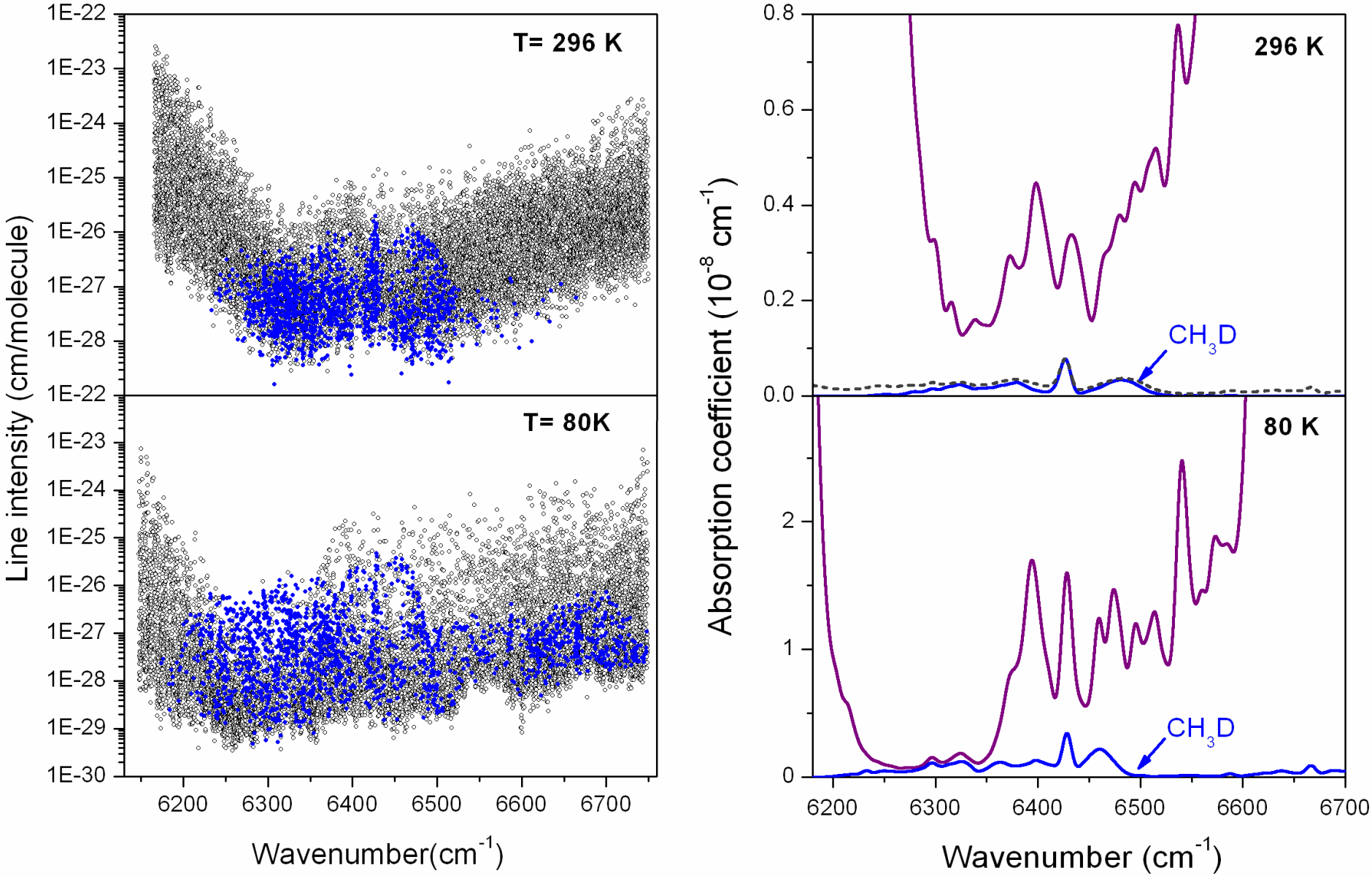
T= 296 K
T= 80K
Line intensity (cm/molecule)
1E-22
1E-23
1E-24
1E-25
1E-26
1E-27
1E-28
1E-29
1E-30
6200
6300
6400
6500
6600
6700
Wavenumber(cm-1)
296 K
80 K
CH3D
CH3D
Absorption coefficient (10-8 cm-1)
0.8
0.6
0.4
0.2
0.0
2
1
0
Wavenumber (cm-1)

Fig.7

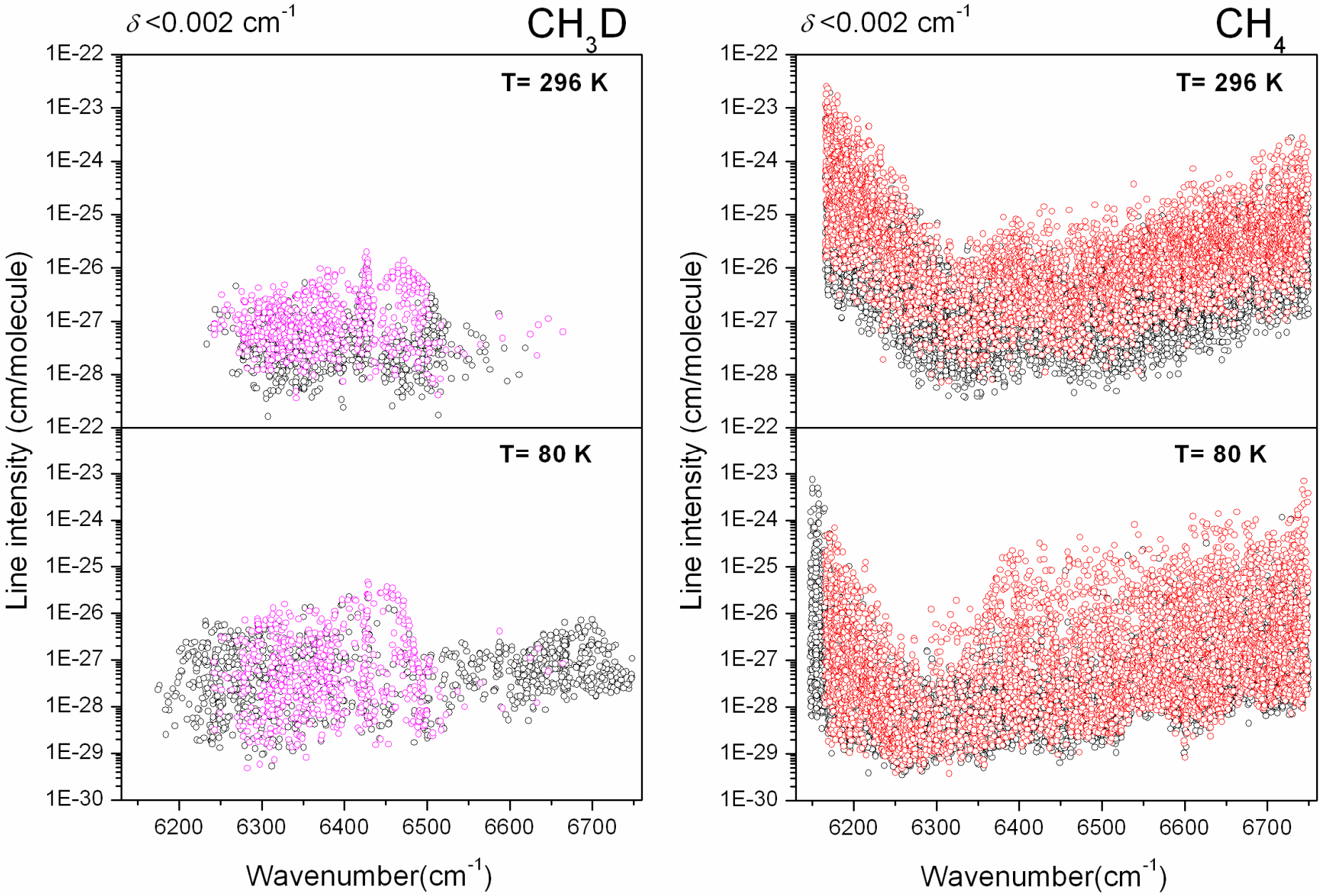
δ <0.002 cm-1
CH3D
T= 296 K
T= 80 K
δ <0.002 cm-1
CH4
T= 296 K
T= 80 K
Line intensity (cm/molecule)
Wavenumber(cm-1)
1E-22
1E-23
1E-24
1E-25
1E-26
1E-27
1E-28
1E-29
1E-30
6200
6300
6400
6500
6600
6700

Fig.8

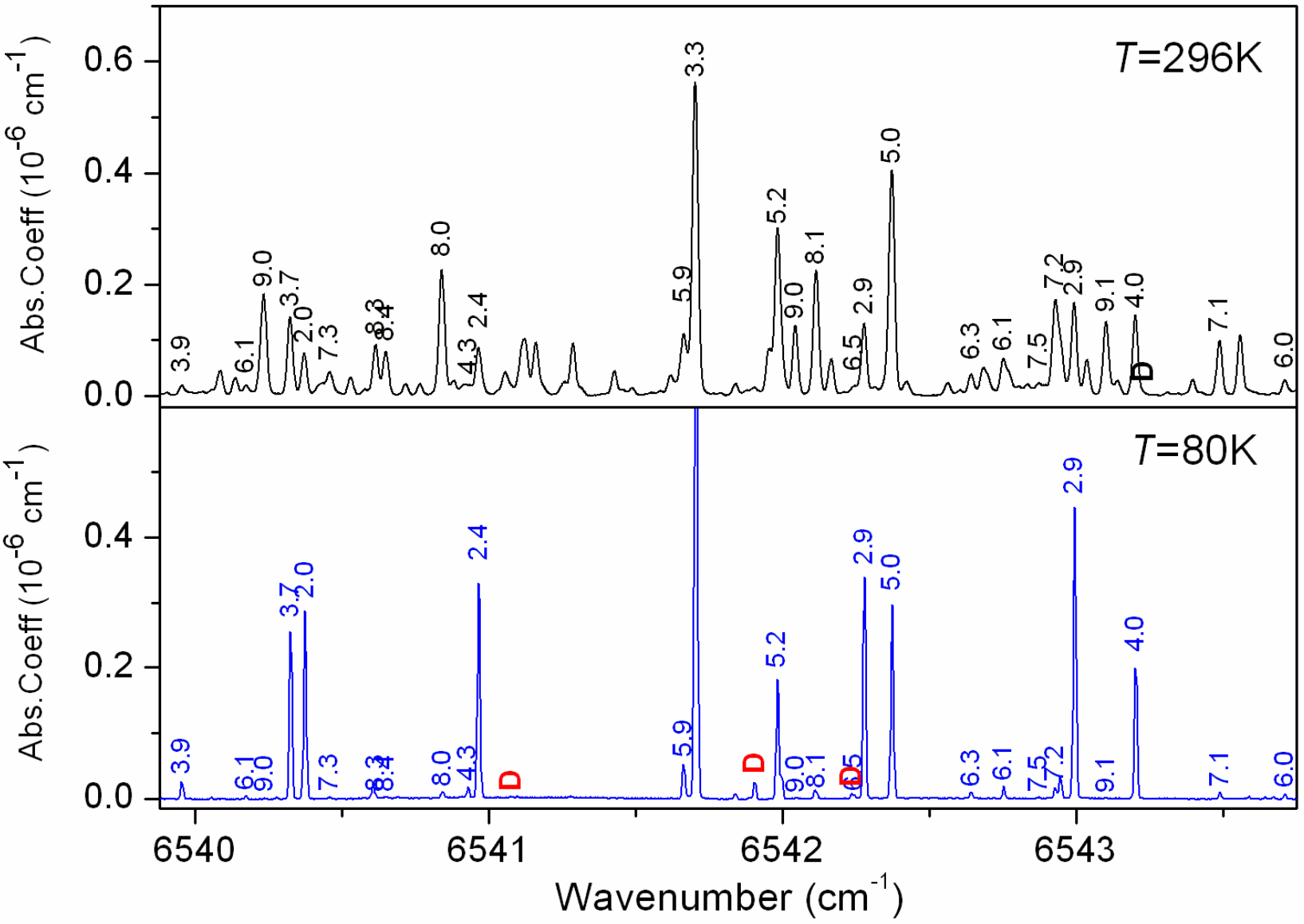
T=296K
T=80K
Abs.Coeff (10^-6 cm^-1)
Wavenumber (cm^-1)
0.0
0.2
0.4
0.6
6540
6541
6542
6543
3.9
6.1
9.0
3.7
2.0
7.3
8.3
8.4
8.0
4.3
2.4
D
5.9
3.3
5.2
9.0
8.1
6.5
2.9
5.0
6.3
6.1
7.5
7.2
2.9
9.1
4.0
7.1
6.0

Fig.9

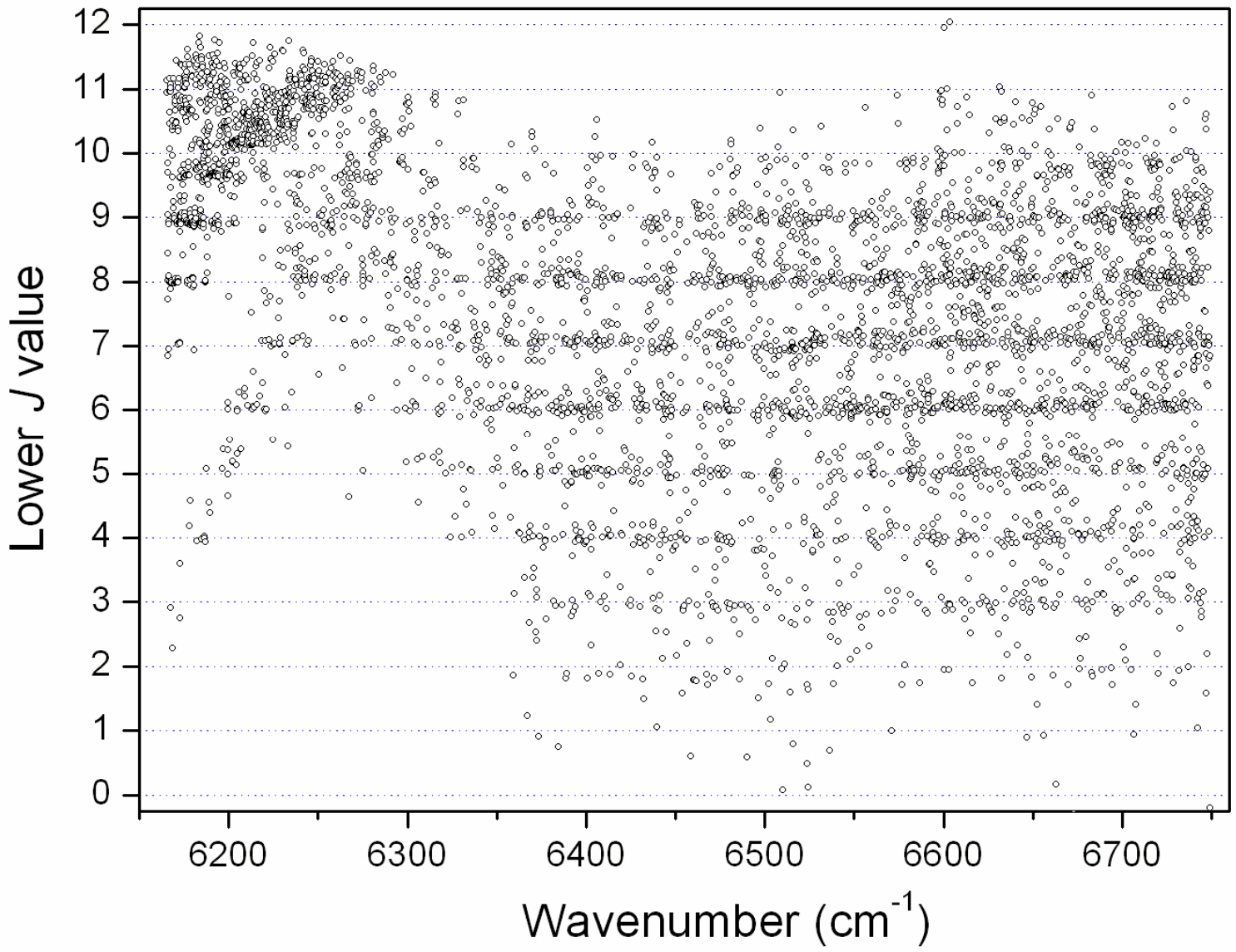
Lower J value
0
1
2
3
4
5
6
7
8
9
10
11
12
6200
6300
6400
6500
6600
6700
Wavenumber (cm-1)

Fig.10

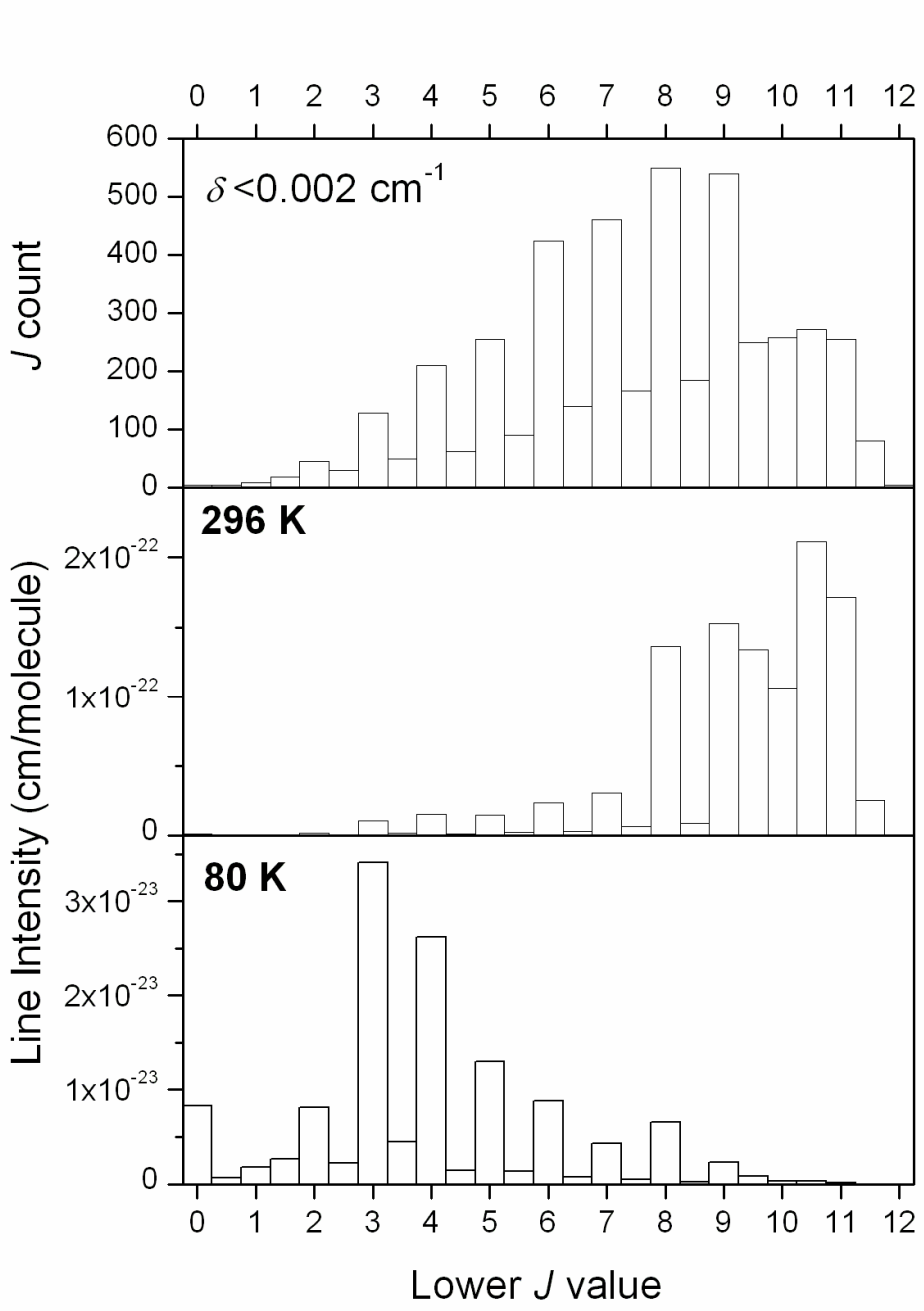
0 1 2 3 4 5 6 7 8 9 10 11 12
600
500
400
300
200
100
0
J count
δ <0.002 cm-1
296 K
2x10-22
1x10-22
0
80 K
3x10-23
2x10-23
1x10-23
0
0 1 2 3 4 5 6 7 8 9 10 11 12
Line Intensity (cm/molecule)
Lower J value

Fig.11

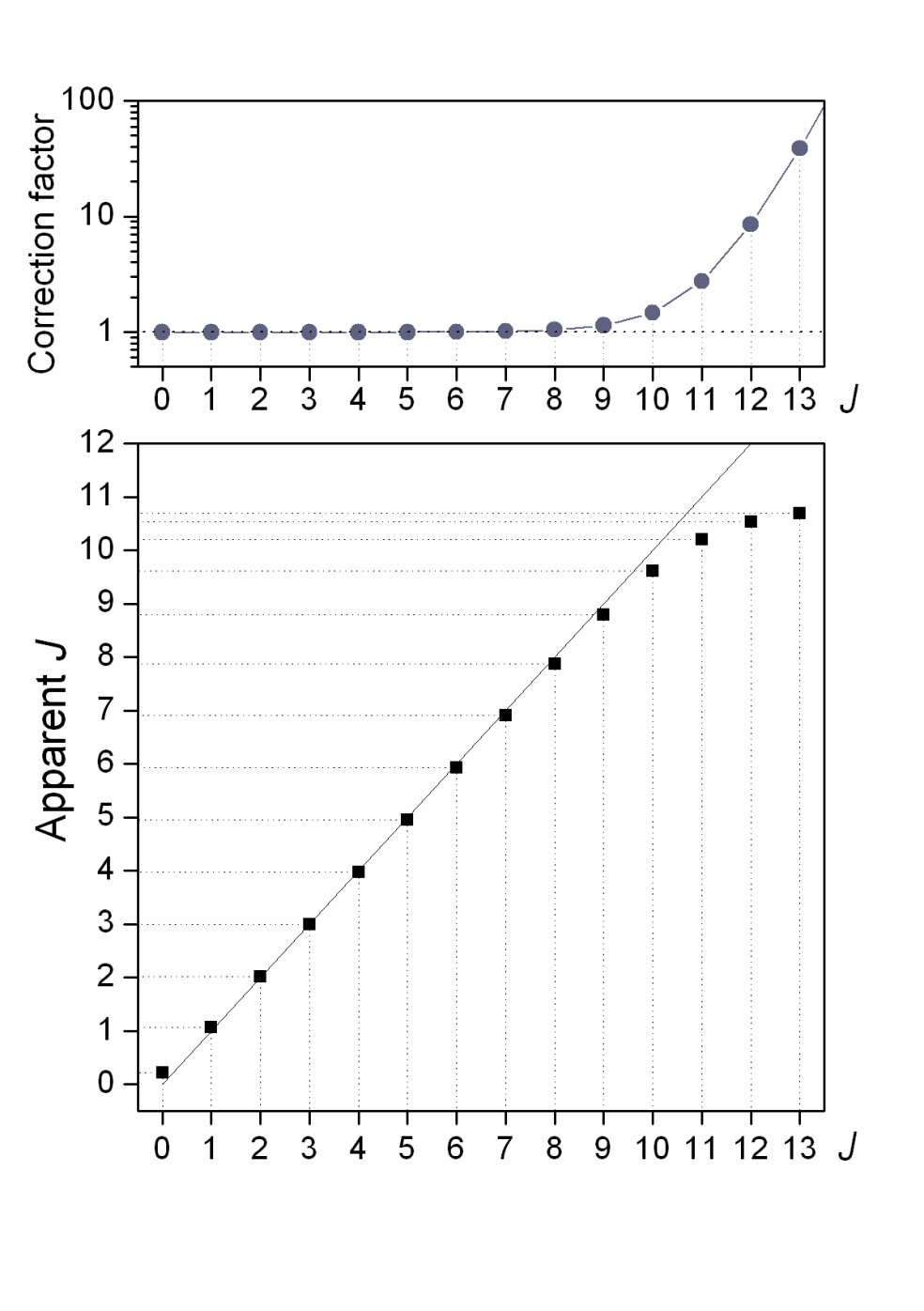
Correction factor
100
10
1
0 1 2 3 4 5 6 7 8 9 10 11 12 13 J
Apparent J
12
11
10
9
8
7
6
5
4
3
2
1
0
0 1 2 3 4 5 6 7 8 9 10 11 12 13 J

Fig.12

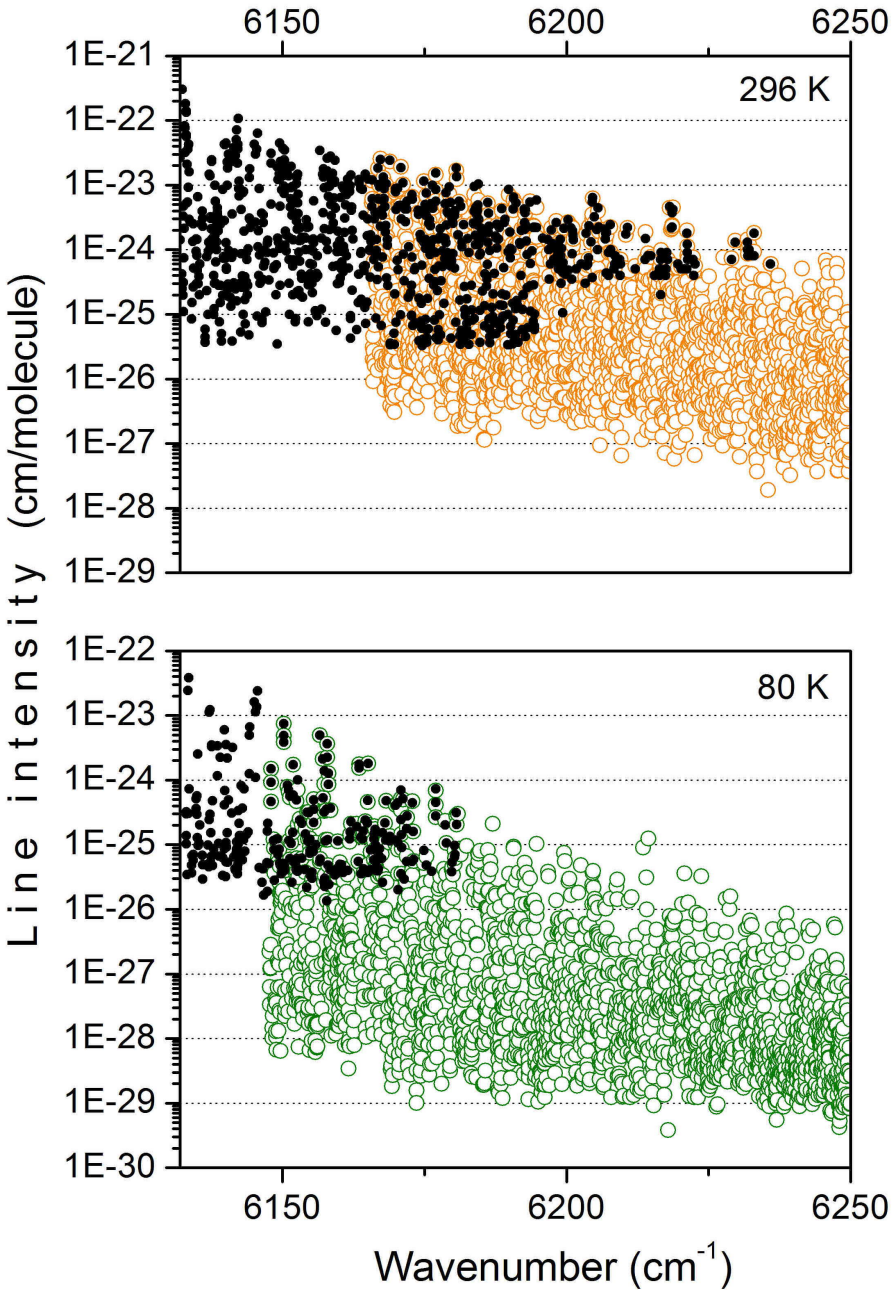
6150
6200
6250
1E-21
1E-22
1E-23
1E-24
1E-25
1E-26
1E-27
1E-28
1E-29
296 K
1E-22
1E-23
1E-24
1E-25
1E-26
1E-27
1E-28
1E-29
1E-30
80 K
Line intensity (cm/molecule)
Wavenumber (cm-1)

Fig.13

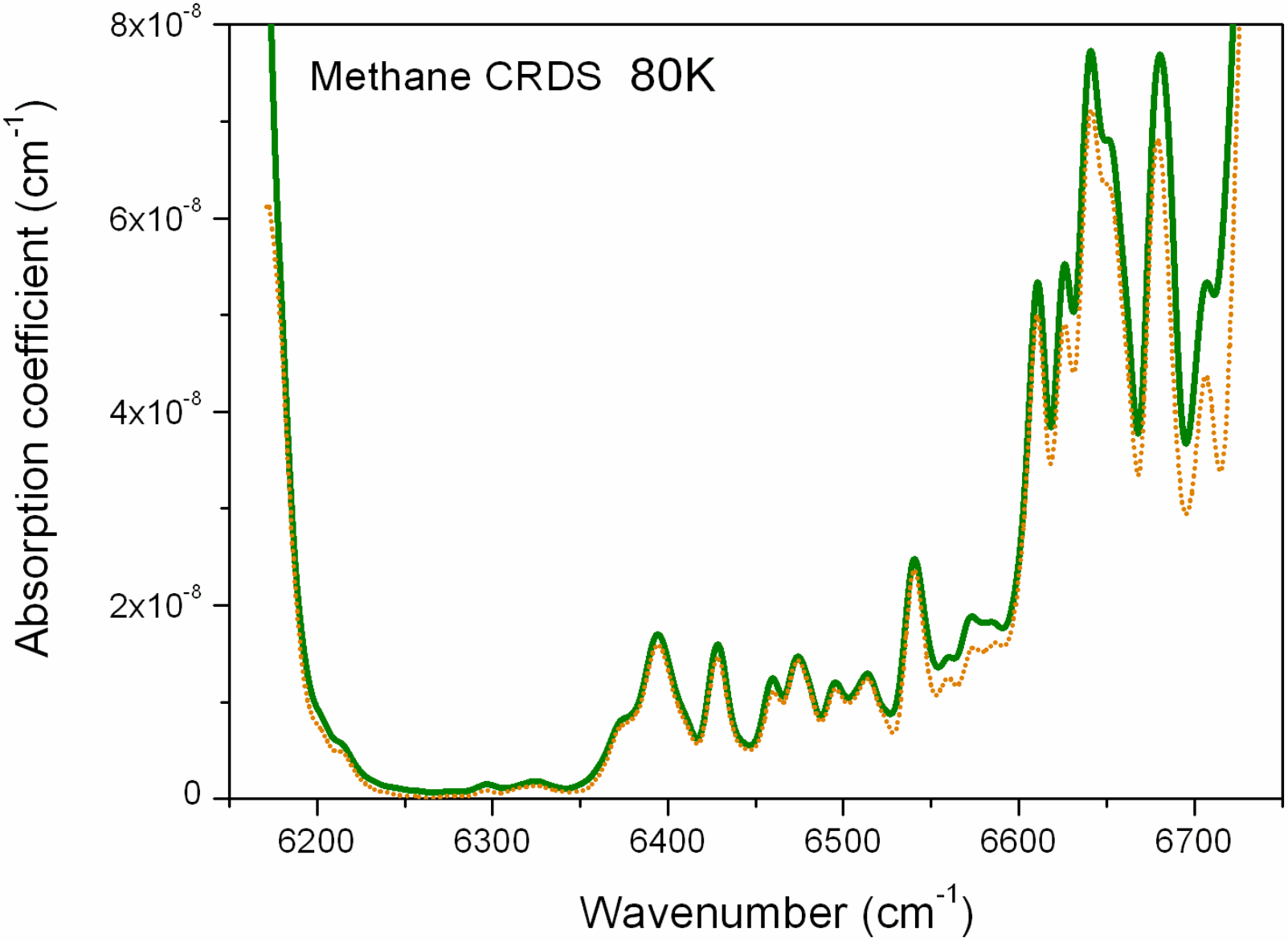
Methane CRDS 80K
Absorption coefficient (cm-1)
8x10-8
6x10-8
4x10-8
2x10-8
0
6200
6300
6400
6500
6600
6700
Wavenumber (cm-1)

e-component, for online publication only

Click here to download e-component, for online publication only: WKC-80K_6165-6750_july23.TXT

e-component, for online publication only

Click here to download e-component, for online publication only: WKC-297K_6165-6750_july23.TXT